NASA/TM-20250004035

9- by 15-Foot Low-Speed Wind Tunnel Commissioning Test Using Advanced Ducted Propulsor

David B. Stephens and David M. Elliott
Glenn Research Center, Cleveland, Ohio

John A. Gazzaniga
HX5, LLC, Brook Park, Ohio

July 2025

NASA STI Program Report Series

Since its founding, NASA has been dedicated to the advancement of aeronautics and space science. The NASA scientific and technical information (STI) program plays a key part in helping NASA maintain this important role.

The NASA STI program operates under the auspices of the Agency Chief Information Officer. It collects, organizes, provides for archiving, and disseminates NASA's STI. The NASA STI program provides access to the NTRS Registered and its public interface, the NASA Technical Reports Server, thus providing one of the largest collections of aeronautical and space science STI in the world. Results are published in both non-NASA channels and by NASA in the NASA STI Report Series, which includes the following report types:

- TECHNICAL PUBLICATION.
  Reports of completed research or a major significant phase of research that present the results of NASA programs and include extensive data or theoretical analysis. Includes compilations of significant scientific and technical data and information deemed to be of continuing reference value. NASA counterpart of peer-reviewed formal professional papers but has less stringent limitations on manuscript length and extent of graphic presentations.

- TECHNICAL MEMORANDUM.
  Scientific and technical findings that are preliminary or of specialized interest, e.g., quick release reports, working papers, and bibliographies that contain minimal annotation. Does not contain extensive analysis.

- CONTRACTOR REPORT.
  Scientific and technical findings by NASA-sponsored contractors and grantees.

- CONFERENCE PUBLICATION.
  Collected papers from scientific and technical conferences, symposia, seminars, or other meetings sponsored or cosponsored by NASA.

- SPECIAL PUBLICATION.
  Scientific, technical, or historical information from NASA programs, projects, and missions, often concerned with subjects having substantial public interest.

- TECHNICAL TRANSLATION.
  English-language translations of foreign scientific and technical material pertinent to NASA's mission.

Specialized services also include organizing and publishing research results, distributing specialized research announcements and feeds, providing information desk and personal search support, and enabling data exchange services.

For more information about the NASA STI program, see the following:

- Access the NASA STI program home page at http://www.sti.nasa.gov

NASA/TM-20250004035

9- by 15-Foot Low-Speed Wind Tunnel Commissioning Test Using Advanced Ducted Propulsor

David B. Stephens and David M. Elliott
Glenn Research Center, Cleveland, Ohio

John A. Gazzaniga
HX5, LLC, Brook Park, Ohio

National Aeronautics and
Space Administration

Glenn Research Center
Cleveland, Ohio 44135

July 2025

Acknowledgments

This work was supported by the NASA Advanced Air Transport Technology project of the Advanced Air Vehicles Program.

This work was sponsored by the Advanced Air Vehicles Program
at the NASA Glenn Research Center.

Level of Review: This material has been technically reviewed by technical management.

This report is available in electronic form at https://www.sti.nasa.gov/ and https://ntrs.nasa.gov/

NASA STI Program/Mail Stop 050
NASA Langley Research Center
Hampton, VA 23681-2199

9- by 15-Foot Low-Speed Wind Tunnel Commissioning Test Using Advanced Ducted Propulsor

David B. Stephens and David M. Elliott
National Aeronautics and Space Administration
Glenn Research Center
Cleveland, Ohio 44135

John A. Gazzaniga
HX5, LLC
Brook Park, Ohio 44142

Summary

A subscale model of an aircraft engine fan was tested in the 9- by 15-Foot Low-Speed Wind Tunnel at the NASA Glenn Research Center in 2022. The fan model was the Advanced Ducted Propulsor Fan 1 designed by Pratt & Whitney in the 1990s. It has been part of multiple wind tunnel test campaigns over the last 30 years. The 2022 test served two purposes: to commission the wind tunnel for fan and propulsor testing after a test facility improvement project and to generate a new data set with the latest data systems and processing improvements. This report documents the test and provides highlights of the aerodynamic and acoustic data that was generated. A supplemental data package that includes several parts (TM-20250004035-SUPPL.zip) accompanies this report.

Data Rights

Nomenclature

8×6 SWT	8- by 6-Foot Supersonic Wind Tunnel
9×15 LSWT	9- by 15-Foot Low Speed Wind Tunnel
ADP	advanced ducted propulsor
CAD	computer aided design
COBRA	Collect, Observe, Broadcast, Record, and Analyze data system program
ESCORT	facility data system program for 9×15 LSWT
FTEB	fan trailing edge blowing
GTF	geared turbofan
IBC	improved bond composite
OTR	over-the-rotor
rpmc	corrected revolutions per minute
UHB	ultra high bypass
VFEN	variable fan exit nozzle

Introduction

An extensive upgrade to the 9- by 15-Foot Low Speed Wind Tunnel (9×15 LSWT) at NASA Glenn Research Center (GRC) was conducted between 2016 and 2019 (Refs. 1 and 2). During this period, the mechanical, hydraulic, pneumatic, control, and data systems for testing scale model aircraft propulsor fans were completely removed and replaced. Much of the original equipment had been accumulated and developed over decades of fan testing. Given the extensive amount of new equipment being implemented simultaneously, it was agreed that the first fan test campaign in the upgraded facility would have to accept some risk. A short-duration commissioning test using an existing, previously tested, NASA-owned fan model was determined as the best way to demonstrate safe operation and accurate data collection.
The 22-in.- (0.559-m-) diameter Advanced Ducted Propulsor (ADP) Fan 1 was designed by Pratt and Whitney in the early 1990s. It is a high-bypass-ratio, low-noise, and variable pitch blade fan model, reconfigurable for a variety of wind tunnel tests. Reports from the previous test have been published on performance (Ref. 3), acoustics (Ref. 4), and noise predictions (Ref. 5). Figure 1 shows the ADP fan test in 1995. Figure 2 shows the same fan model in the renovated test section during 2022.

Figure 1.—Advanced Ducted Propulsor fan test in 1995 (NASA Image C-1995-1896).

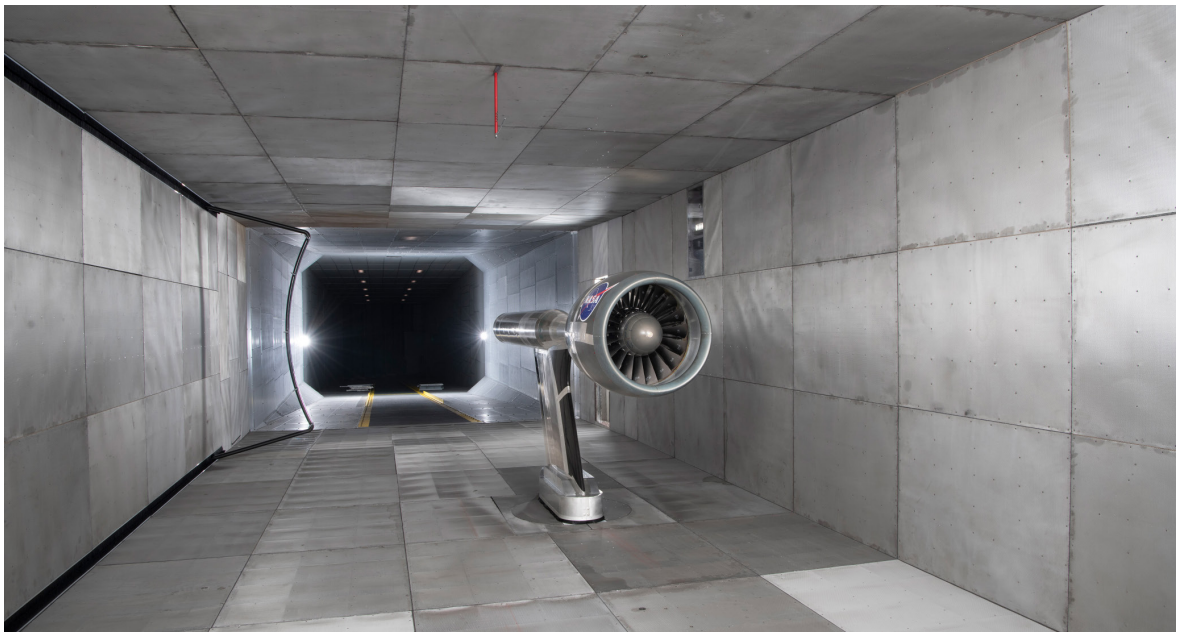

Figure 2.—Advanced Ducted Propulsor fan test in 2022 (NASA Image GRC-2022-C-04039).

Testing Powered Fan Models

Fan testing in the NASA Glenn 9×15 LSWT generally utilizes the NASA Ultra High Bypass (UHB) drive rig (Ref. 6), a four-stage turbine driven by heated compressed air. A wide variety of fan models have been tested on this system over the decades. It offers flexible and powerful capabilities, usable for landing and takeoff testing in the 9×15 LSWT and for cruise testing in the 8- by 6-Foot Supersonic Wind Tunnel (8×6 SWT). The UHB rig is mounted on a turntable on the floor of the 9×15 LSWT, so the model can be turned in the horizontal plane to represent an in-flow angle of attack into the fan model, although this was not used in the 2022 test. Extensive pressure and temperature instrumentation is embedded throughout the fan model, which is described in an instrumentation manual developed to accompany the test. Some sensors are integral and flush-mounted with the flow surfaces; others are part of rakes that span the flow passage. Fan blades can be instrumented for aeromechanics evaluation and tip clearance instrumentation is frequently installed. Measurements external to the fan are also used, including upstream flow rakes and a traversing sideline microphone system.

Each test conducted in the 9×15 LSWT is assigned a unique number associated with the facility data system program used for the test. Prior to 2019, this system was named ESCORT and the names started with a “D.” The new data system program is called COBRA (for Collect, Observe, Broadcast, Record, and Analyze) and the program names start with a “C.”

ADP Fan 1 Hardware

The 22-in. ADP test hardware has been used in several fan tests in the 9×15 LSWT, which is a testament to the flexibility and robustness of the model. These tests are summarized in Table 1. The commissioning test used existing hardware in a baseline configuration, with flight inlet and nozzle and no acoustic liners. This configuration was tested during parts of the ESCORT programs D051 in 1995, D054 in 1996 to 1997 and D065 in 2005. The ADP core hardware has been used for additional Pratt & Whitney fan testing, including the recent geared turbofan (GTF) entries that were part of the ERA/FAA CLEEN program from 2012 to 2015 (Ref. 7). A cross section of the ADP Fan CAD model is shown in Figure 3.

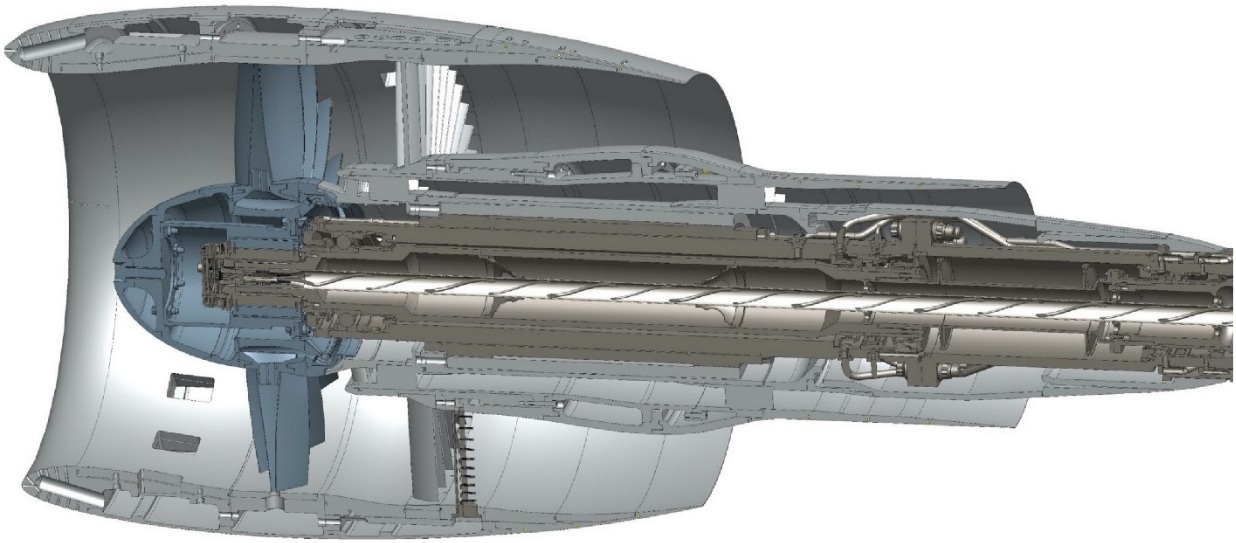

Figure 3.—CAD model of ADP tunnel hardware. Forward part of UHB drive rig is shown in dark gray.

TABLE 1.—ADP TEST ENTRIES

Program name	Test dates	Description
ESCORT D051	1995	First test of ADP Fan 1, including the original composite blade set (which failed upon testing), the IBC blade set (which did not fail) and a titanium blade set (also did not fail). These blades have a spherical tip shape and variable pitch. The VFEN was used to map fan performance. These blades all had 0.055 in. (1.40 mm) of tip clearance
ESCORT D054	1996 to 1997	Fan 1 (IBC) was tested with three different kinds of liners in multiple bays on the model. A second fan (ADP Fan 2) was tested for acoustic performance and mapped with the VFEN. Fan 2 was found to be less successful than Fan 1 and had not been used since.
ESCORT D065	2005	FTEB and Aft Splitter test. New, thicker hollow blades were built for air injection, along with a solid set for comparison. These blades have a smaller tip gap (0.020 in. (0.51 mm)) and are not variable pitch. A new hardwall rubstrip was built to accommodate the cylindrical tip shape. Separately, another set of variable pitch Fan 1 IBC blades was tested with 0.020 in. (0.51 mm) clearance.
ESCORT D070	2008	OTR and Soft Vane technology maturation test. The FTEB blades were used, along with a new set featuring nickel metal coated tips (to be used with some kind of experimental tip clearance sensor). Both of these blade sets were damaged by operating near the perforated OTR acoustic treatment. The Fan 1 0.055 in. (1.40 mm) clearance blades were also run during this test entry.
COBRA C003	2022	Commissioning test for improved 9×15 LSWT. Used ADP Fan 1 hardware with 0.020 in. tip clearance blade set in best effort to repeat D065 data set. Subject of present report.

Fan Blades

The label “ADP fan” is not unique and has been used by both NASA and Pratt & Whitney to refer to several fans tested through the years, including a 17-in.- (0.432-m-) diameter model used in the NASA Glenn 8×6 SWT and a large model used in the NASA Ames Research Center 40×80 National Full-Scale Aerodynamics Complex. Even at the 22-in.-diameter scale tested at NASA Glenn, multiple fan models are generically called “ADP fan.” See Table 2 for a list of the fan blades built for the 22-in. ADP fan model. The fan tested during commissioning testing is the Low Noise Research Fan Stage Design described in a contractor report of the same name by Pratt & Whitney (Ref. 8). It is also sometimes called “ADP Fan 1” because a follow-on “Fan 2” design was built and tested in the 1990s. The ADP Fan 1 fan

stage has 18 rotor blades, 45 stator blades, and 63 core inlet guide vanes. The 0.055-in. tip clearance test represents an end-of-life condition while the 0.020-in. tip clearance is a beginning-of-life condition. The Fan 1 and Fan 2 blades are variable pitch for improved aerodynamic efficiency throughout changing flight conditions and also for reverse thrust.

The fan tested in 2022 is the ADP Fan 1 IBC with 0.020-in. tip clearance, which is listed in the last row of Table 2. This is a composite blade set built circa 1995, but the tips were not cut to shape until the D065 test. These blades were previously run in November 2005 as part of D065. This blade set requires the baseline hardwall rubstrip (ca. 1995) that is machined for the variable pitch blade set. The blades were set to the take-off pitch setting of –9°, which has been the most commonly tested configuration. The stator set tested was the original 45-vane set (ca. 1995). The fan model with the 0.020-in. blades tested in 2005 is shown in Figure 4. This is the configuration repeated for the 2022 test.

TABLE 2.—SETS OF FAN ROTOR BLADES AVAILABLE FOR ADP 22-in. MODEL

Fan blades	Notes
Fan 1 titanium, 0.055-in. (1.40-mm) tip clearance	Built and tested in 1995
Fan 1 composite, 0.055-in. (1.40-mm) tip clearance	Built in 1995, disintegrated during testing
Fan 1 IBC, 0.055-in. (1.40-mm) tip clearance	Built as replacement and used in 1996
Fan 2 titanium	Different blade design
FTEB composite	Based on Fan 1 design, not variable pitch, hollow
Fan 1 IBC, 0.020-in. (0.51-mm) tip clearance	Extra blades built for 1996 test. Tip cut later to design clearance. Used during parts of D065 (in 2005) and for the present test C003 (in 2022)

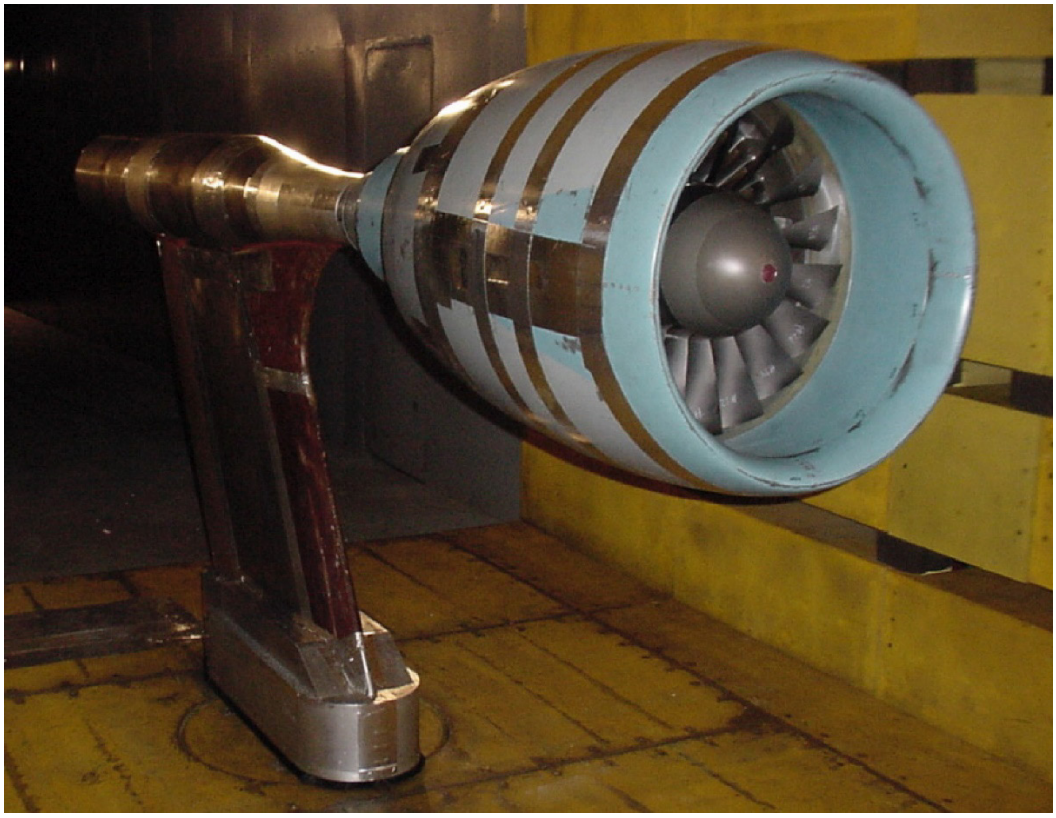

Figure 4.—ADP Fan 1 in 9×15 LSWT in November 2005, 0.020-in. tip gap, test D065, runs 20 and 21.

Blade Vibration Testing

The rotor blade vibration characteristics were measured as part of the safety preparations for this test. Because the blades were made more than two decades earlier, there was some uncertainty regarding their structural integrity. A nondestructive testing method called laser holography was used to quantify the structural properties of the fan blades. Measurements were made of each blade to determine vibratory mode shapes and frequencies. These results were compared with each other, and with laser holography measurements made in 2004. The 2004 measurements were on blades manufactured during the same period but not on the 0.020-in. (0.51-mm) tip gap blades. The very small difference in blade length was not expected to meaningfully affect the vibration characteristics. Testing in 2004 was performed at NASA Glenn (Figure 5). Testing in 2018 (Figure 6) was performed by Laser Technology, Inc. of Norristown, Pennsylvania.

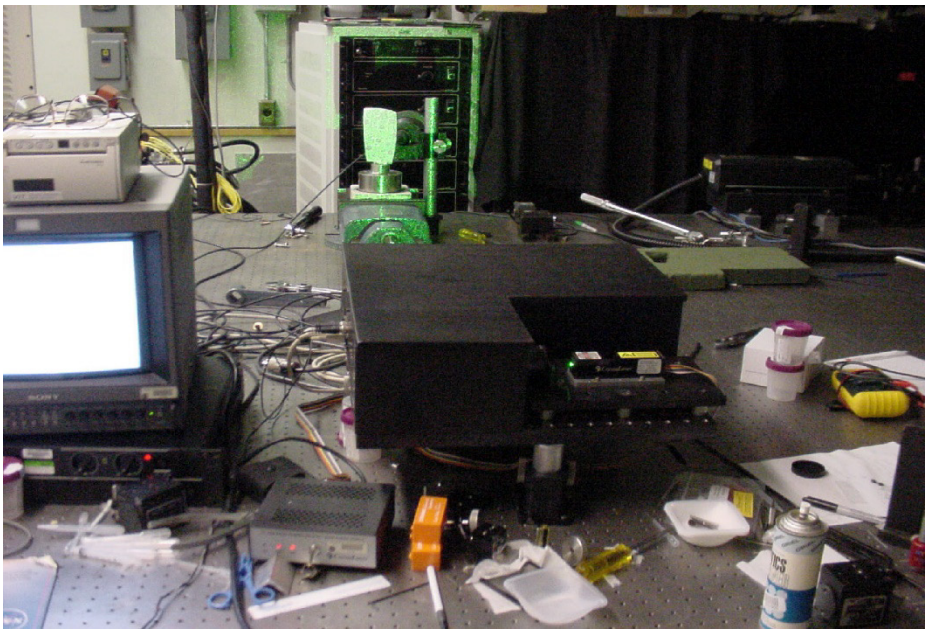

Figure 5.—Holography testing in 2004 at NASA Glenn.

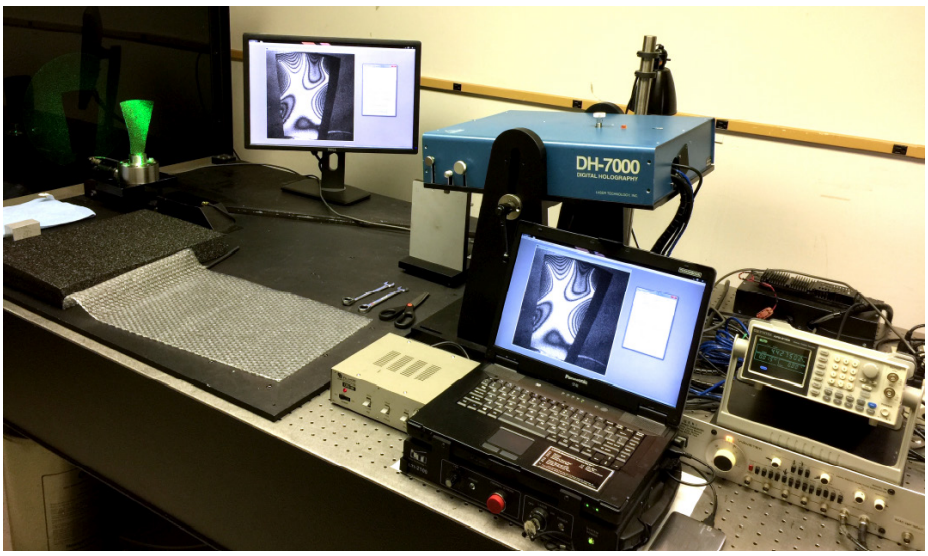

Figure 6.—Holography test setup in 2018 at Laser Technology, Inc.

Figure 7 to Figure 10 compare images from 2004 with those from 2018 of the first four mode shapes and vibration frequencies. The mode shapes and frequencies were found to agree well enough that no major damage to the composite bonding was suspected. Had any issues occurred during testing, the vibration characteristics of the blades could have contained important information to review.

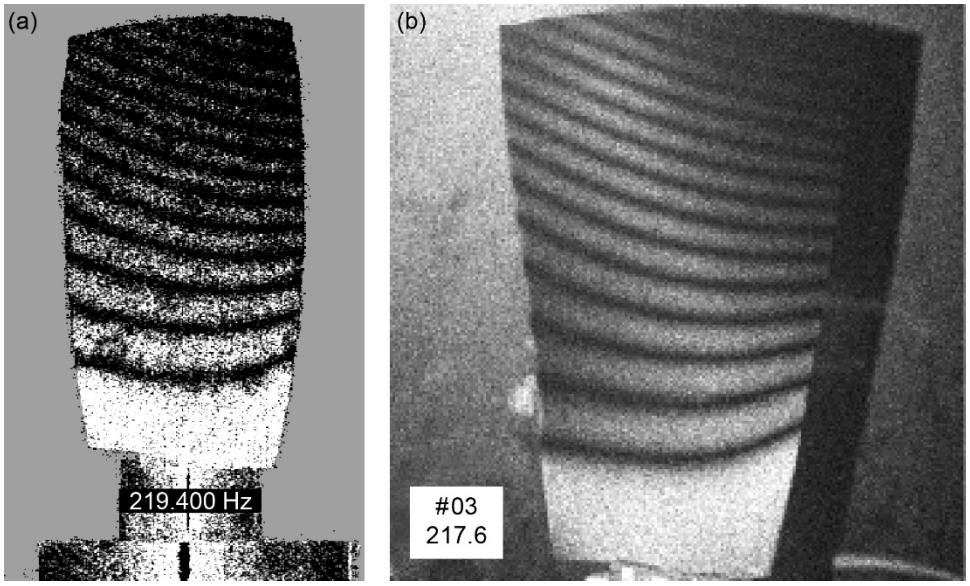

Figure 7.—Mode shape 1. (a) 2004 image. (b) 2018 image.

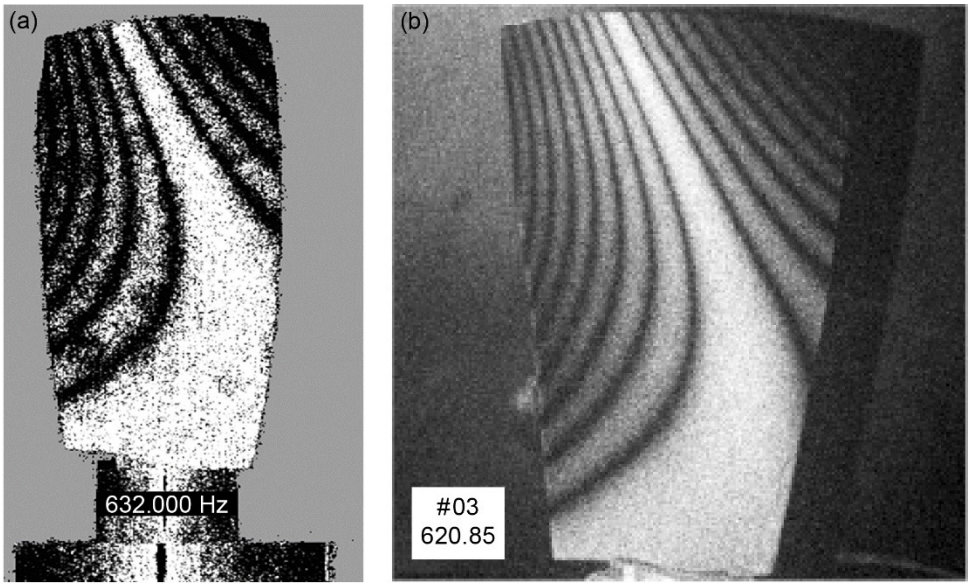

Figure 8.—Mode shape 2. (a) 2004 image. (b) 2018 image.

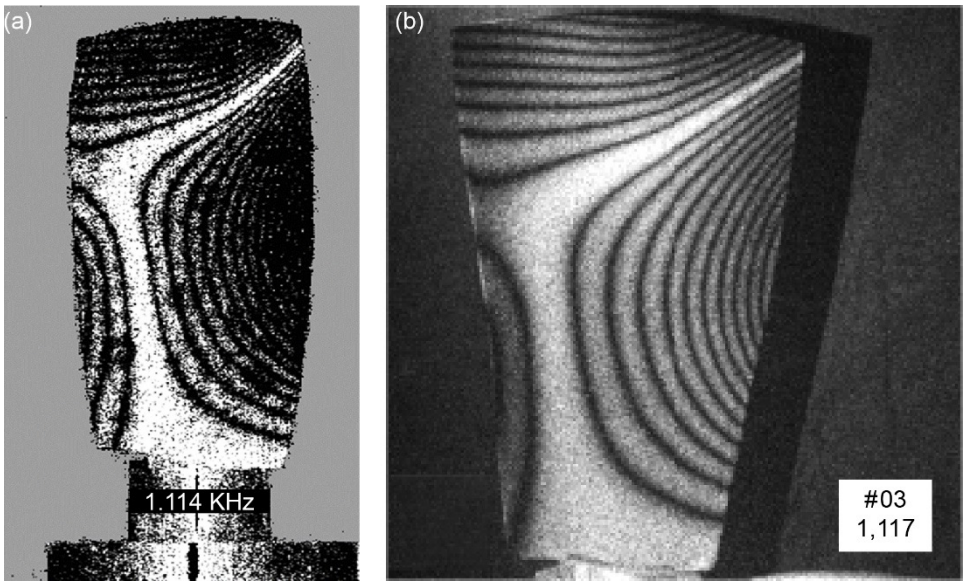

Figure 9.—Mode shape 3. (a) 2004 image. (b) 2018 image.

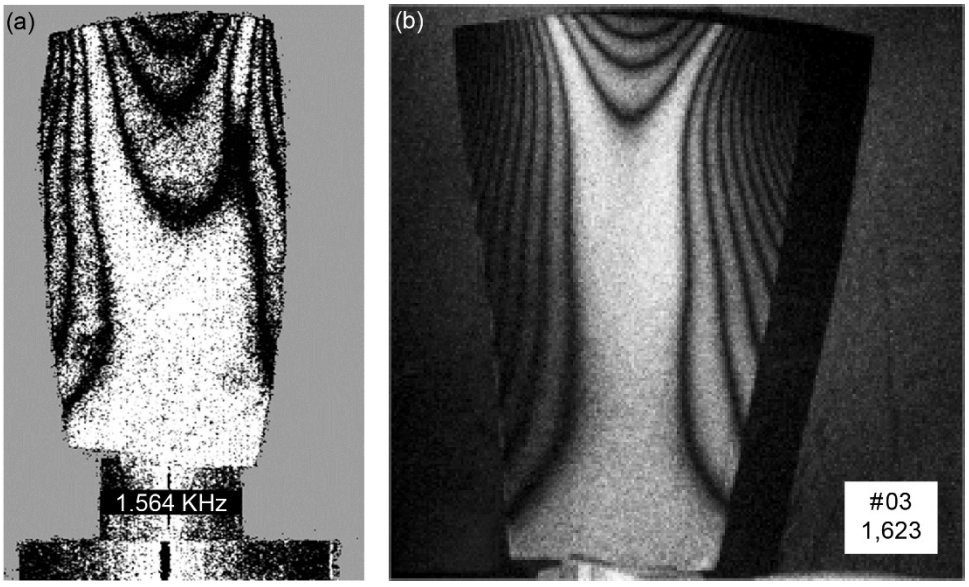

Figure 10.—Mode shape 4. (a) 2004 image. (b) 2018 image.

The frequencies of the first four modes were compared with two prior test results, as shown in Figure 11. Note that the scale is focused around a value of 1.000. These were normalized by the average of the three measurements. Measurements of modes 1 and 2 were about 1 percent lower in 2018, while mode 4 was 1.5 percent higher. The 2018 measurement was made on the longer 0.020-in. (0.51-mm) blades, which perhaps explains the lower mode 1 and 2 vibration frequency. These measurements were deemed close enough that the blades were safe to test. Individual vibration maps were also compared and no outliers were identified. Two of the fan blades each had a small chip missing from a tip trailing edge, so these were designated as the spares because it was necessary to build an 18-blade fan from 20 available blades.

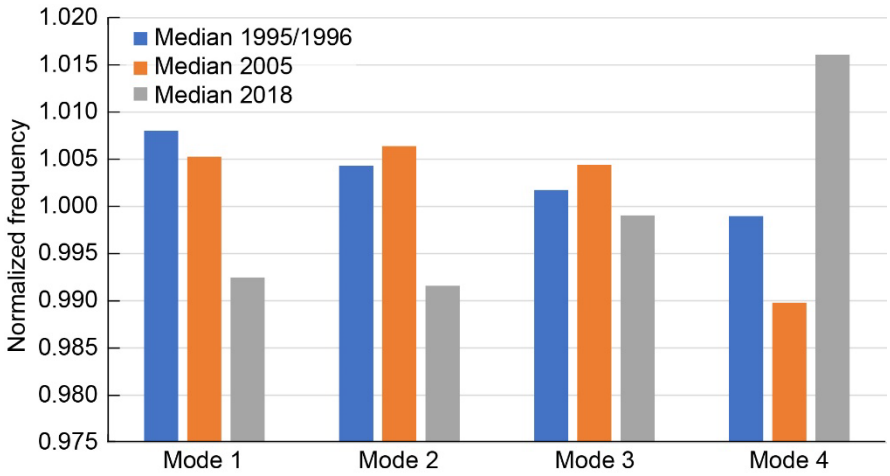

Figure 11.—Historical mode frequency results.

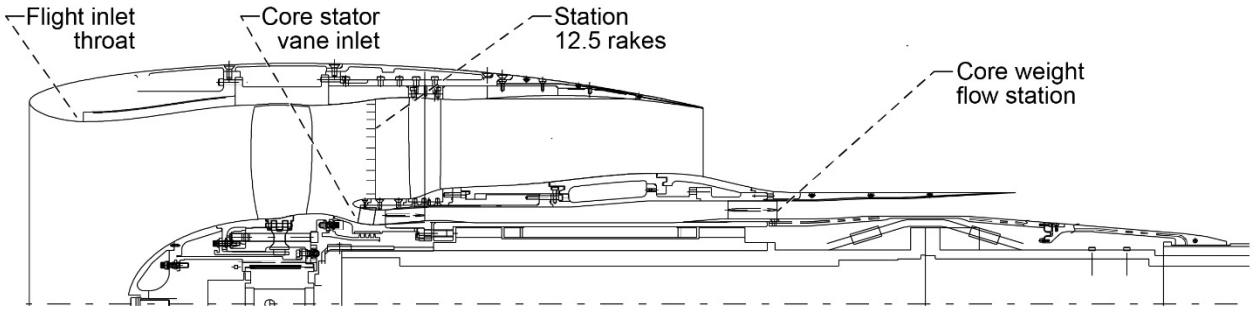

Figure 12.—Aerodynamic performance instrumentation locations in fan model.

Performance Instrumentation

The commissioning test discussed in this report used a typical set of fan aerodynamics instrumentation, principally high-channel-count steady temperature and pressure sensors. Including the sensors required for safe operation of the UHB drive rig and the wind tunnel, the test utilized a total of 60 temperature and 236 pressure channels. Three key instrument locations are used to determine the fan stage performance. Station 12.5 is between the rotor and the stator in the bypass duct; the core stator vane inlet location is downstream from the fan and uses instrumented vanes; the core weight flow station is downstream in the core duct. From the test instrument manual, the rake locations and diagram are given in Figure 12. A comprehensive list of measurement points and geometric locations can be found in Figure 3 to Figure 5 of an existing report (Ref. 3).

Fan performance in terms of pressure and temperature rise and adiabatic efficiency was determined from total pressures and total temperatures measured by the station 12.5 rakes and fan duct wall static pressures. The model total weight flow (also called mass flow) was determined using static pressures located at the flight inlet throat with a previously developed correlation equation. Core weight flow was determined from pressures and temperatures rakes in the core duct. Core aerodynamic performance was obtained from the core stator vane leading-edge-mounted instrumentation.

The station 12.5 rakes were the newest set, which were built for the 2008 (D070) test. These were inspected and checked for instrument damage and calibrated in the CE-12 Free Jet Probe Calibration Facility at NASA Glenn (Ref. 9). The fan model showing station 12.5 rakes is pictured in Figure 13. Note that the rakes are angled to account for the swirl expected from the counter-clockwise rotation of the fan when forward looking aft. The instrumented core stator vanes are partially visible.

An upstream aerodynamic rake known as the cruciform rake is shown in Figure 14. This probe measures the streamtube upstream of the fan model and is used to reduce uncertainty in the temperature of the flow going into the fan in case the tunnel flow is thermally stratified to a meaningful degree.

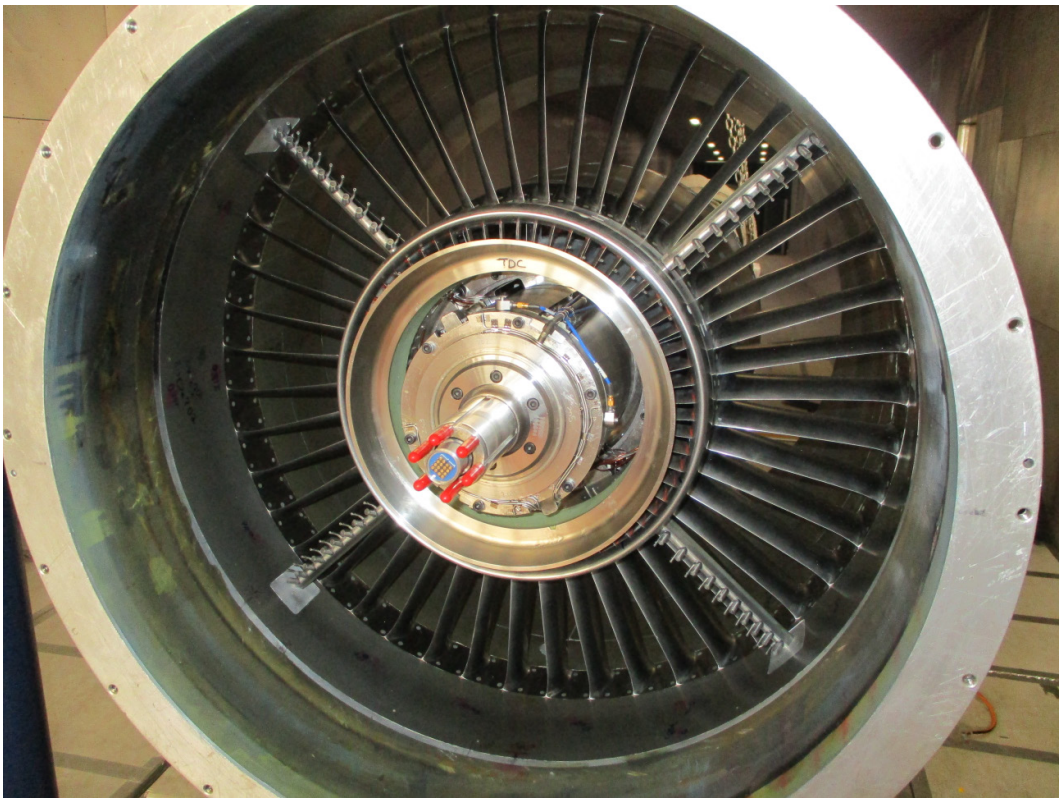

Figure 13.—Station 12.5 rakes shown during model buildup.

Figure 14.—Fan model and cruciform rake.

Acoustic Microphone Traverse

A traversing microphone has been used in the 9×15 LSWT for decades to acquire acoustic data on a sideline. This measurement represents a simulated flyover, where the observer is moving past a stationary source, rather than a moving source and a stationary observer. The microphone system, in use since 1986, consisted of a screw-drive mechanism mounted to the floor of the test section that allowed movement of the traversing microphone probe. The screw drive was covered by thin aluminum covers that were angled in such a way as to divert reflections up and away from the microphones on the probe. This method was not ideal, in that the lower microphones on the traverse were closer to the drive mechanism, thereby measuring any flow noise over this mechanism. Additionally, the entire drive system of the traversing microphone probe was in the flow of the tunnel. Fixed microphones were typically placed in the aft of the test section to collect downstream radiated sound, as this is often a dominant radiation direction for high-bypass fan models. A pair of fixed microphones upstream of the model were installed for a 2012 test with Pratt & Whitney and have been in regular use since then. A typical instrumentation for the 2010s is shown in Figure 15.

Figure 15.—Microphone layout used for 2014 Honeywell test.

A new in-flow microphone measurement system was developed to accompany the upgraded 9×15 LSWT test section. It was decided to utilize the open space outside the upper and lower corners on one wall of the test section to contain the drive motors for a new traversing microphone system. An airfoil shape similar to the old traversing probe was used and would enter the test section from the corners through brush seals. The angle of the strut entering the test section was chosen such that it would transition through the boundary layer of the floor and ceiling quickly to reduce noise due to turbulence interaction. To keep the vertical section of the probe at a constant radius from the centerline of the model, the entire probe is in the shape of the letter "M" rotated 90° in the clockwise direction looking downstream. This allowed the placement of five microphones on the new traversing probe as opposed to three on the old probe. The distance from the model centerline was maintained at 89 in., the same distance as the old probe. The design is shown in Figure 16.

The new traversing probe was manufactured of carbon fiber composite by Wolf Composites, Columbus, Ohio. The same Brüel & Kjær Type 4939 ¼-in. microphones with FITE (Flow Induced Tone Eliminator) nosecones were used as before. To keep all flow surfaces small and reduce changes in diameter, GRAS 26AC-1 ¼-in. preamplifiers were used rather than the ¼-in. to ½-in. adapters used previously. Cables from the preamplifiers to the signal conditioning units outside of the tunnel were 5-pin LEMO to 7-pin LEMO. The mounting of the microphones to the traverse utilized tubes and fairings to keep the flow smooth. The microphone installation process was done with precision to ensure no rough surfaces were present.

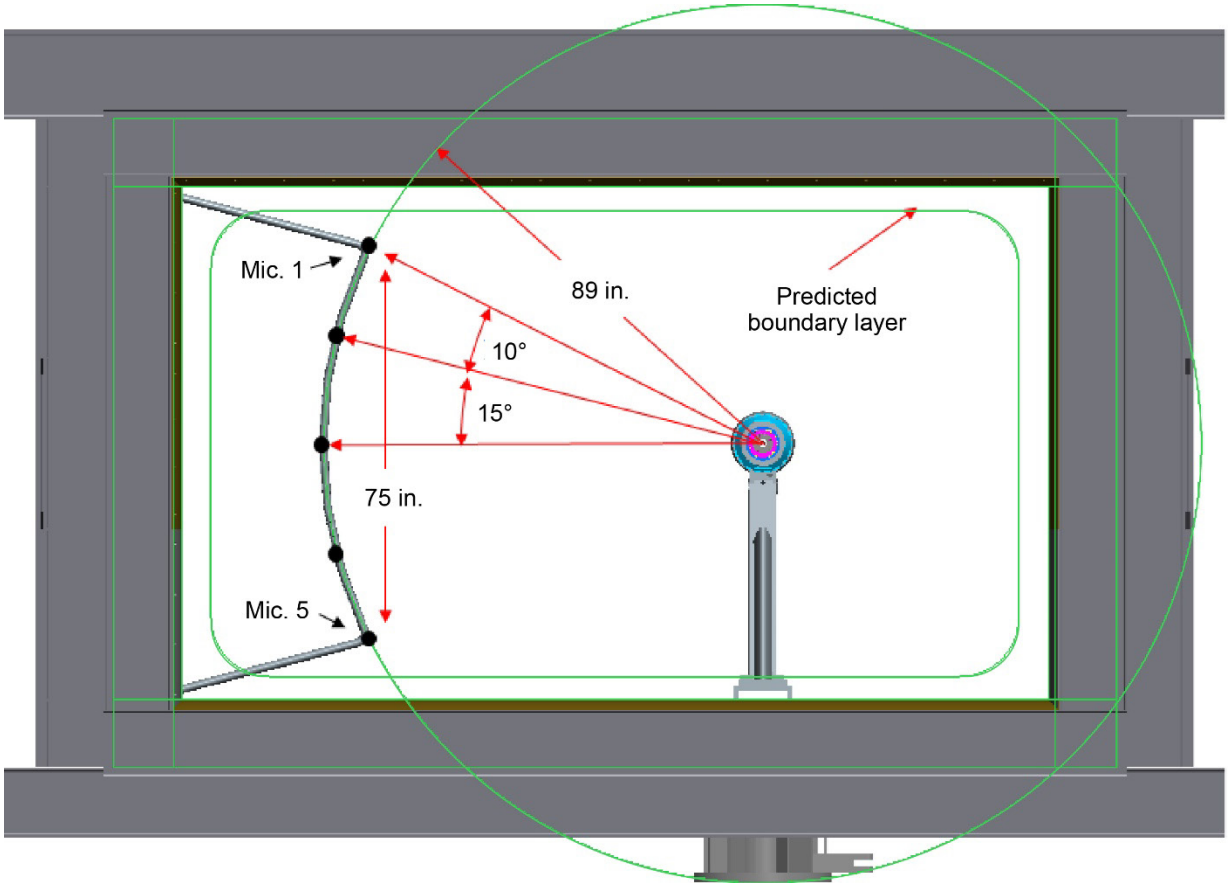

Figure 16.—New traverse design and sensor geometry looking downstream.

The drive system of the new microphone probe consists of two separate drive carriages located at the top and bottom corners outside the test section connected by a belt drive. Kollmorgen 120 V motors, Harmonic Drive® (HD Systems, Inc.) gearing, and Temposonics magnetic position sensors are used to provide movement and position indexing of the traverse. The traverse operation is accomplished using a Galil® (Galil Motion Control, Inc.) controller through Wonderware® (Aveva Software, LLC) software. The linear travel of the traversing probe is 360 in. with an accuracy of 0.008 in/ft.

This new traversing design accomplishes the objectives of removing the drive system from within the test section, which should reduce potential flow noise. The upper and lower halves of the traverse are mirror images of each other, thereby eliminating the instance of having the lower microphone adjacent to the drive mechanism and increasing the chance of contamination with additional flow noise. The new belt-drive system is also inherently quieter than the old screw-drive mechanism.

The lengthened test section enables a longer traverse path than was previously possible, specifically allowing for more downstream angles. As shown in Figure 17, the center microphone nominally moves from 167 in. downstream of the fan stacking axis to 187 in. upstream. The five microphones together sweep out a sector of a cylinder.

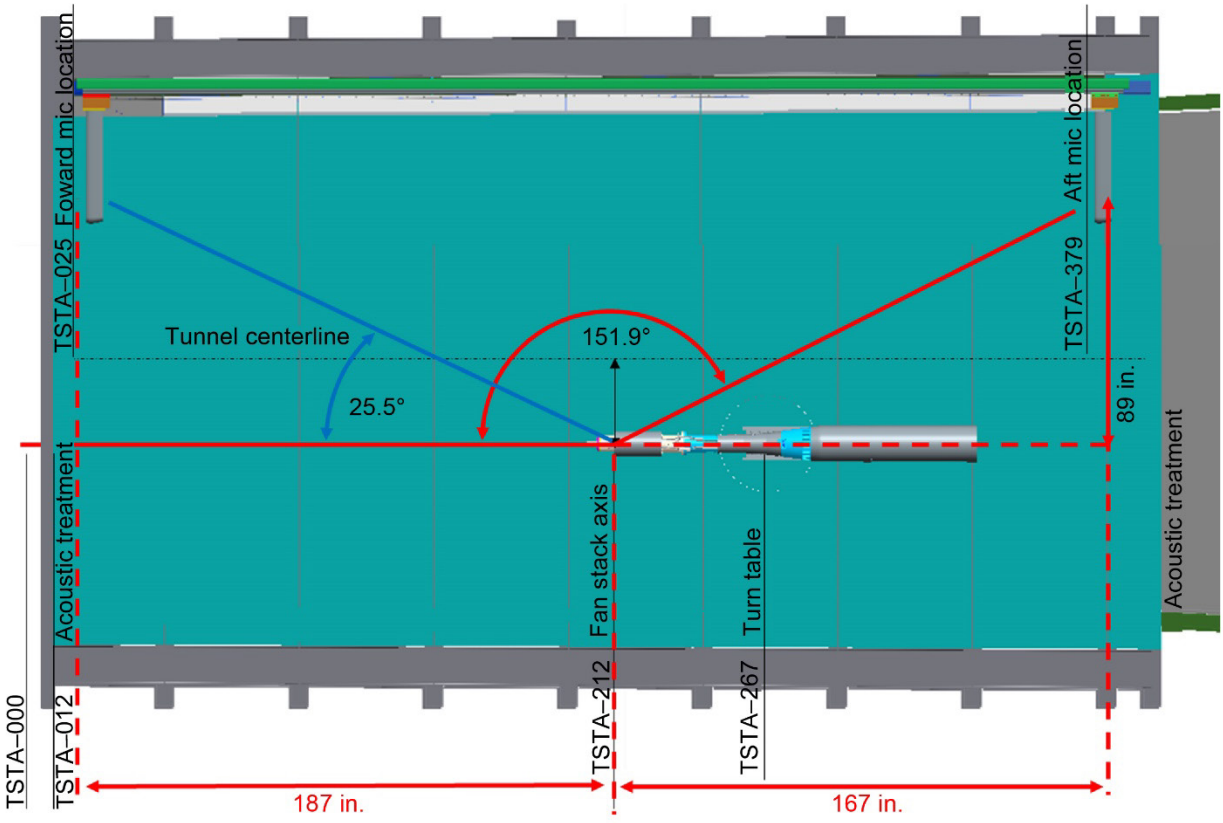

Figure 17.—Traverse sideline geometry extent in design drawings.

Microphone Instrumentation

A total of seven microphones were used to measure radiated sound during the ADP 2022 test described in this report, including the new five-sensor traversing microphone and two microphones forward of the fan model. The microphones on the traverse are numbered 1 to 5 from top to bottom, forward ceiling and floor microphones are 6 and 7 respectively. The functionality of the three aft floor microphones previously used was replaced by the new, longer, traversing microphone. The traversing microphone rake and forward microphones are shown in Figure 18, and the traversing microphone arm was also shown on the left side of Figure 2. The ceiling microphone installation interfered with the upstream cruciform rake and was removed when not in use. The floor microphone has been identified as a severe tripping hazard and is only installed just before testing. The microphones are all externally polarized using LEMO cable runs from the 9×15 LSWT's Auxiliary Control Room to the test section. Brüel & Kjær Nexus™ signal conditioning amplifiers provided the excitation voltage for the microphones and the unsteady pressures were recorded on an R.C. Electronics DataMAX system. The microphone electronics and software were not updated from that used in prior testing (Ref. 10). The new Modicon PLC system was used to control the new traversing microphone arm and trigger the data recorder. A diagram of the workflow is shown in Figure 19.

Figure 18.—Microphones. (a) Traversing microphone rake. (b) Forward microphone.

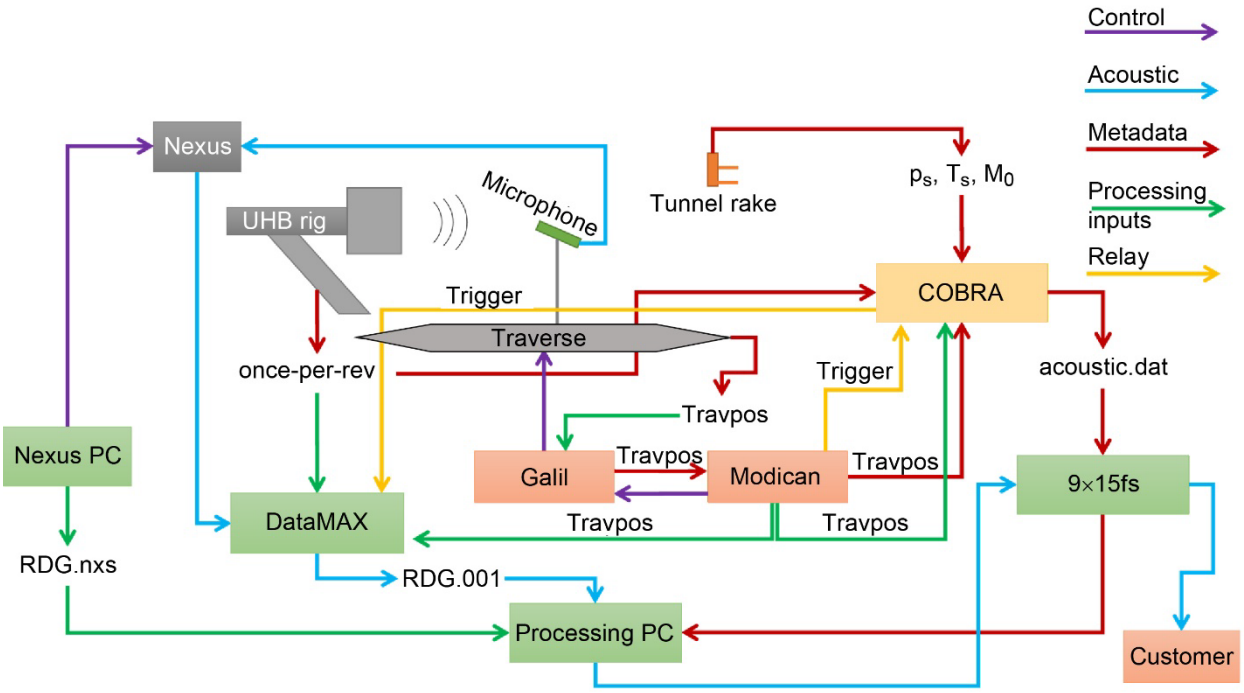

Figure 19.—Acoustic data workflow.

Test Matrix

The commissioning testing program was intended to be concise while also verifying the new fan model control, safety, and data systems. The wind tunnel control system had previously been validated during empty wind tunnel testing in Spring 2020. The main data to be acquired was aerodynamic performance and acoustic measurements for comparison with the 2006 data. This resulted in a very short test matrix with just two configurations. An aerodynamic configuration included the 12.5 rakes; the acoustic configuration did not. The instrumentation in the station 12.5 rakes was carried off the model into a tube that was fastened to the tunnel floor, as seen in Figure 20. The tube is needed because there was not enough space to get the number of pressure tubes and thermocouple wires off the model via the center shaft. The instrument tube was removed along with the rakes for the acoustic portion of the test. The variable pitch blades were set to the takeoff pitch angle of –9° for this test and associated geometry files.

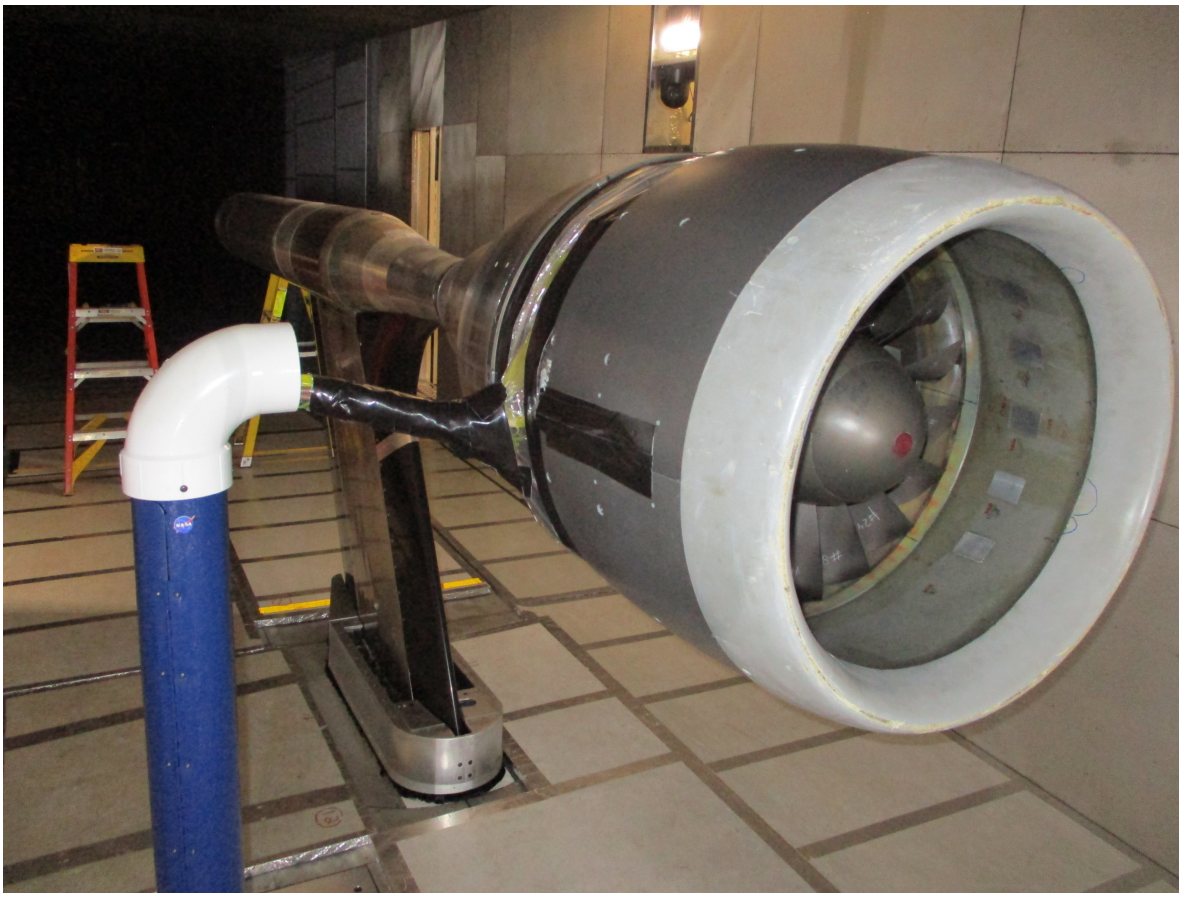

Figure 20.—Instrument tube used as cable run for taking wires and tubes off outer duct.

Run Summary

The completed test matrix is shown in Table 3. Runs 0-A through 0-J were used to check out the fan drive rig control system. Run 1 was the aero performance testing and runs 2 and 3 were the acoustic testing. Acoustic testing takes longer because of the need to traverse the microphone array. Run 4 was a checkout of other data systems that might potentially replace the DataMAX recorders. Runs 5 to 7 were to test acoustic performance and vibration characteristics of the drive rig while using two different turbine mufflers. The ADP fan model was removed and runs 8 to 10 were of the bare drive rig by itself, then with two different sound sources installed on it.

Reading Summary

The research portion of the test was planned and executed as a fully populated matrix of 12 fan speeds over four tunnel Mach numbers. The same operating conditions were run for both performance and acoustic configurations. The performance configuration was completed in run 1; the acoustic configuration was split between 2 days, given as run 2 and run 3. The acoustic testing takes longer due to the time required for the traversing microphone to collect data at each point. The individual COBRA readings are given in Table 4. The fan was operated by setting the corrected shaft speed, $rpmc = rpm/\sqrt{\theta}$, where θ is the total temperature of the air in the wind tunnel divided by the standard day temperature. This corrects for the different work done by the fan at different air density.

TABLE 3.—COMPLETED TEST MATRIX

[For all runs, the rig angle of attack (AoA) = 0°. Thermocouple ports on ceiling rakes taped for all runs except 1 and 4.]

Run	COBRA readings	Data type	Date	Mach	Cruciform rake[a]	Sta. 12.5 rakes[b]	Comments
0-A	66-69	Checkout	27-May-22	Static	In	In	
0-B	70-74	Checkout	31-May-22	Static	In	In	
0-C	76-82	Checkout	1-Jun-22	0.1	In	In	
0-D	87-98	Checkout	2-Jun-22	0.1	In	In	
0-E	99-101	Checkout	3-Jun-22	Static	In	In	
0-F	103-113	Checkout	6-Jun-22	0.1	In	In	
0-G	114-129	Checkout	7-Jun-22	0.1	In	In	
0-H	130-134	Checkout	8-Jun-22	Static	In	In	
0-I	135-151	Checkout	9-Jun-22	0.1	In	In	
0-J	152-164	Checkout	10-Jun-22	0.1, 0.2	In	In	
1	165-231	Performance	13-Jun-22	0.10, 0.15, 0.20, 0.22	In	In	
2	240-309	Acoustic	15-Jun-22	0.10, 0.15	Out	Out	
3	310-377	Acoustic	16-Jun-22	0.20, 0.22	Out	Out	
4	378-423	Acoustic and performance	17-Jun-22	0.1, 0.2, 0.22	In	Out	Acoustic data acquired with three different systems
5	424-470	Acoustic	23-Jun-22	0.10, 0.20	Out	Out	GE muffler installed
6[c]	471-500	Checkout	27-Jun-22	0.1	Out	Out	NASA muffler (re)installed
7[c]	501-506	Checkout	28-Jun-22	0.1	Out	Out	NASA muffler installed
8	507-523	Acoustic	29-Jun-22	0.05, 0.07, 0.10, 0.15, 0.20, 0.22	Out	N/A	Bare drive rig, encased in polymer tube and capped by an aluminum spinner
9	524-529	Acoustic	29-Jun-22	0.1	Out	N/A	Wrapped drive rig, deer whistle on starboard side
10[d]	531-548	Acoustic	30-Jun-22	0.1	Out	N/A	Wrapped drive rig with impinging jet source

[a]With cruciform rake in, the rake is located at model station (MS) 81.25.

[b]For the station 12.5 rakes, “1” means the rake is installed, “0” means that no rake is present.

[c]For runs 6 and 7, the floor microphone is OUT.

[d]For run 10, the impinging jet source is also located on the wrapped rig's starboard side.

TABLE 4.—COBRA READINGS FOR AERODYNAMIC PERFORMANCE AND ACOUSTIC MEASUREMENTS

		Aerodynamic readings				Acoustic readings			
		Tunnel Mach				Tunnel Mach			
% rpmc	rpmc	0.1	0.15	0.2	0.22	0.1	0.15	0.2	0.22
40	3,500	170	185	200	215	245	274	315	346
57	4,950	171	186	201	216	248	276	318	348
62	5,425	172	187	202	217	250	278	323	350
67	5,900	173	188	203	218	253	281	325	352
77	6,700	174	189	204	219	255	285	327	354
80	7,030	175	190	205	220	257	287	329	356
86	7,525	176	191	206	221	259	290	331	358
90	7,900	177	193	207	222	261	293	333	360
95	8,345	178	194	208	223	263	296	335	362
100	8,750	179	195	209	224	265	298	337	364
104	9,100	181	197	211	226	268	302	340	368
108	9,480	182	198	212	227	271	305	343	371

Comparison with Prior Test Data

The ADP fan model represents the quietest fan of this size that is likely to be tested in the 9×15 LSWT. It has a low tip speed and low pressure ratio design, along with a long inlet and large rotor-stator spacing. The only exception to the quiet design features was the relatively large 0.055-in. (1.40-mm) tip gap blade set, which is on top of the larger gap required for a spherical tip cut needed for the variable pitch blades. The more recent tests have used longer fan blades, which are cut to a more nominal 0.020-in. (0.51-mm) tip gap. The wind tunnel improvement project had the main purpose to lower the background noise in the test section, so it made sense to test with the quietest fan model available to demonstrate the new capability. The ADP fan model is also NASA-owned and the data is unrestricted. Finally, this commissioning test would include a limited set of repeat points from a prior test performed during 2005 (D065), allowing for verification of updated instrumentation and computation methods.

The ADP Fan 1 hardware was assembled using the same drawings and procedures developed in 1995 for test campaign D051. The rotor blades were assembled in the same order as in the 2005 test, except for the substitution of blade 12 for blade 11 due to a small chip missing from blade 11. The rest of this section will briefly compare the new data to prior measurements. Test procedures have historically avoided conditions with low signal-to-noise ratio, which could potentially result in bad data. Specifically, testing was conducted with the 9×15 LSWT operating at Mach 0.1 to reduce background noise. The readings from the legacy test are given in Table 5. Note that two readings were required for acoustic measurements using the legacy data system.

Aerodynamics

The focus of the aerodynamic comparison is on the station 12.5 rakes because these are used for computing fan performance. The readings selected for this comparison were 100 percent fan speed and Mach 0.1 tunnel speed, D065 reading 1386 as given in Table 5 and C003 reading 179 as given in Table 4.

The first set of comparisons is the pressure ratio, temperature ratio, and calculated efficiency as a function of radial span. This is the average of each of the 12.5 rakes for a given radius. The pressure ratio agrees to within 0.5 percent of the legacy test, with the largest margin at the hub position, as seen in Figure 21.

TABLE 5.—ESCORT READINGS FROM 2005 (D065) FOR AERODYNAMIC PERFORMANCE AND ACOUSTIC MEASUREMENTS. TUNNEL MACH = 0.1 FOR ALL READINGS LISTED

% rpmc	rpmc	Aerodynamic readings	Acoustic readings
40	3,500	1359	----------
57	4,950	1362	1292 and 1293
62	5,425	1365	1295 and 1296
67	5,900	1368	1299 and 1300
77	6,700	1371	1302 and 1303
80	7,030	1374	1306 and 1307
86	7,525	1377	1309 and 1310
90	7,900	1380	----------
95	8,345	1383	1316 and 1317
100	8,750	1386	1320 and 1321
104	9,100	1389	----------
108	9,480	1392	1327 and 1328

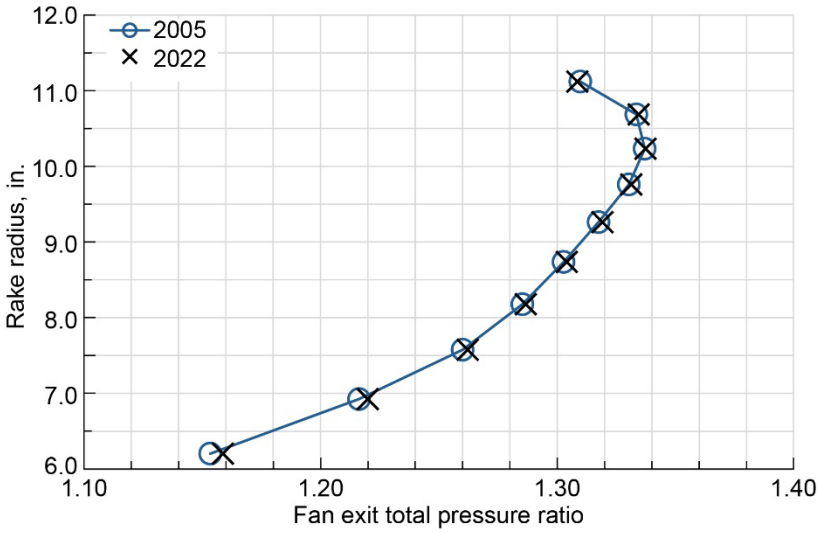

Figure 21.—Radial averaged fan exit total pressure ratio at 100 percent fan speed, Mach 0.1.

The temperature ratio is an even closer match to the legacy data, with variations of only 0.15 percent, with the biggest difference again at the hub, as seen in Figure 22.

The adiabatic efficiency is calculated from the temperature and pressure ratios as

$$\eta = \frac{PR^{\frac{\gamma-1}{\gamma}} - 1}{TR - 1},$$

where PR is the pressure ratio, TR is the temperature ratio, and γ is the ratio of specific heat capacities. The resulting efficiency is plotted in Figure 23. The biggest difference between the two data sets is seen at

the blade tip radius. The trends in temperature and pressure ratio shown previously were in opposite directions, resulting in a 1.1 percent difference in efficiency measured at the blade tip.

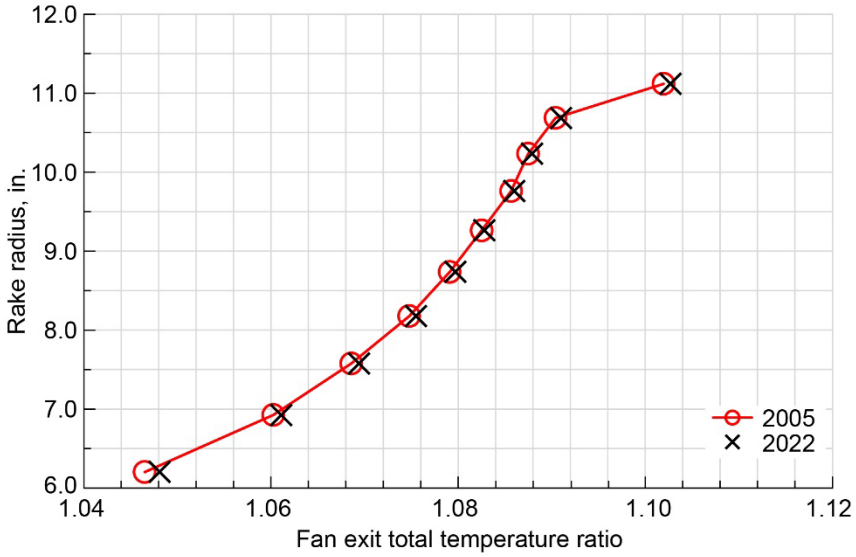

Figure 22.—Radial averaged fan exit total temperature ratio at 100 percent fan speed, Mach 0.1.

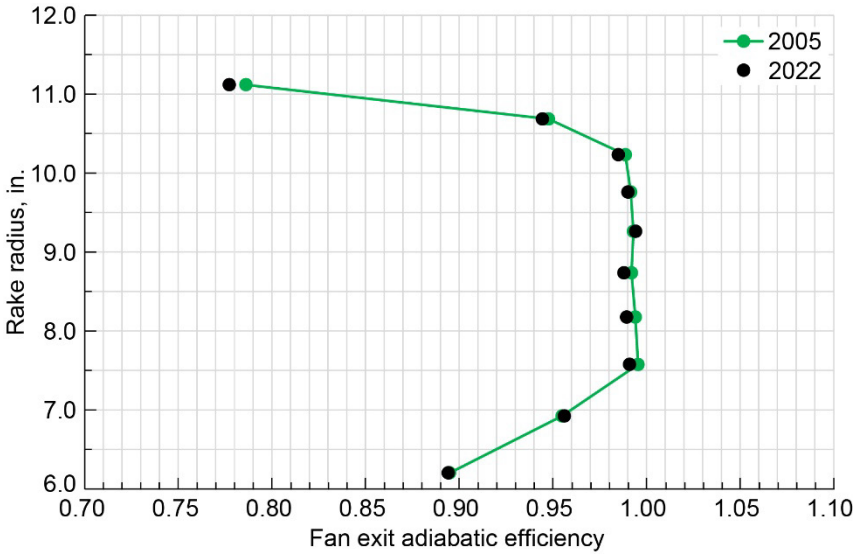

Figure 23.—Radial averaged fan exit adiabatic efficiency at 100 percent fan speed, Mach 0.1.

The pressure ratio measured at each radial station by the 12.5 rakes can be area averaged to give a total fan exit pressure ratio. This result is shown for all fan speeds in Figure 24. The largest difference in pressure was at 95 percent speed, where the measured pressure ratio was 0.14 percent lower in 2022.

Similarly, the fan efficiency is shown in Figure 25. The efficiency was 1.16 percent lower in 2022 at 40 percent speed but agreed to within 0.54 percent on average at other speeds. At 100 percent speed, the difference is only 0.37 percent, which represents excellent agreement between the data sets and is considered satisfactory for a repeat experiment. Compared to prior testing, the rakes were calibrated before the present test for pressure and temperature recovery in the CE-12 Facility. This is a new best-practice and these calibrations were used in the data processing for the C003 test program but not in prior programs such as D065. This could explain some of the observed differences.

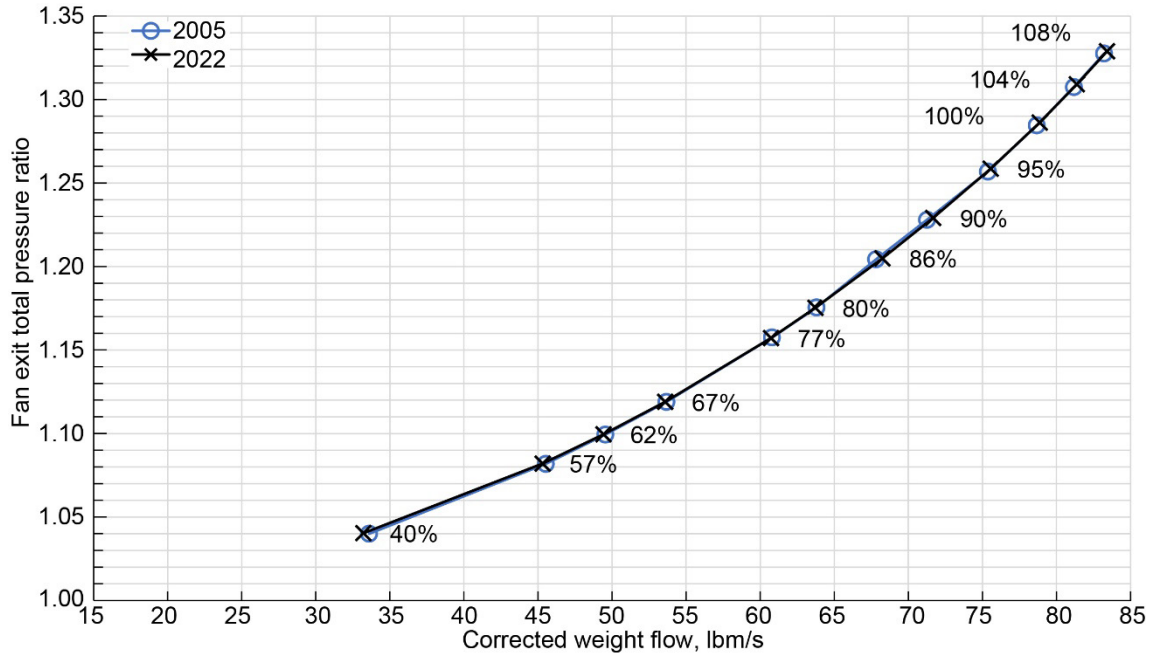

Figure 24.—Fan exit total pressure ratio versus total corrected weight flow. Data labels indicate percent rpmc.

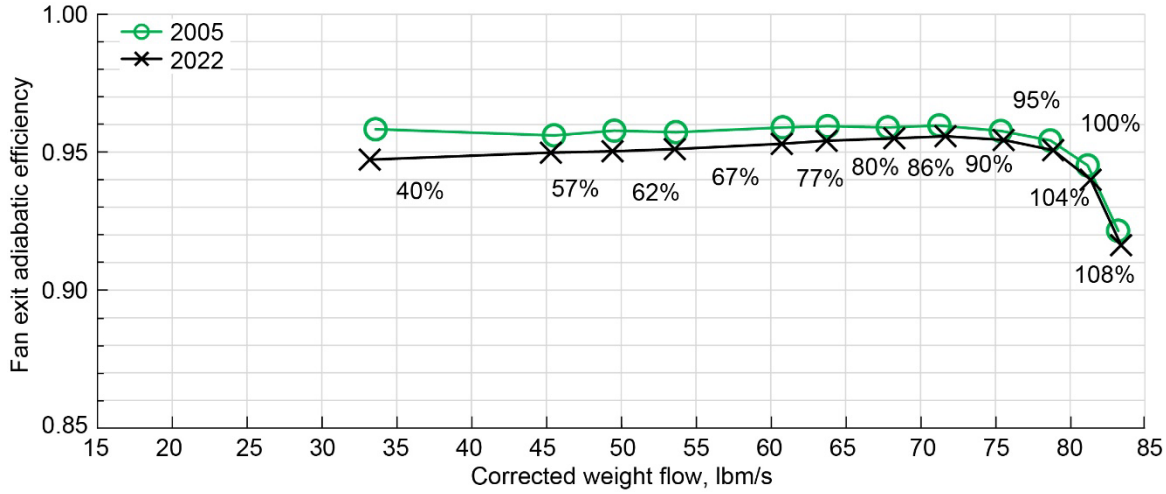

Figure 25.—Fan exit adiabatic efficiency versus total corrected weight flow. Data labels indicate percent rpmc.

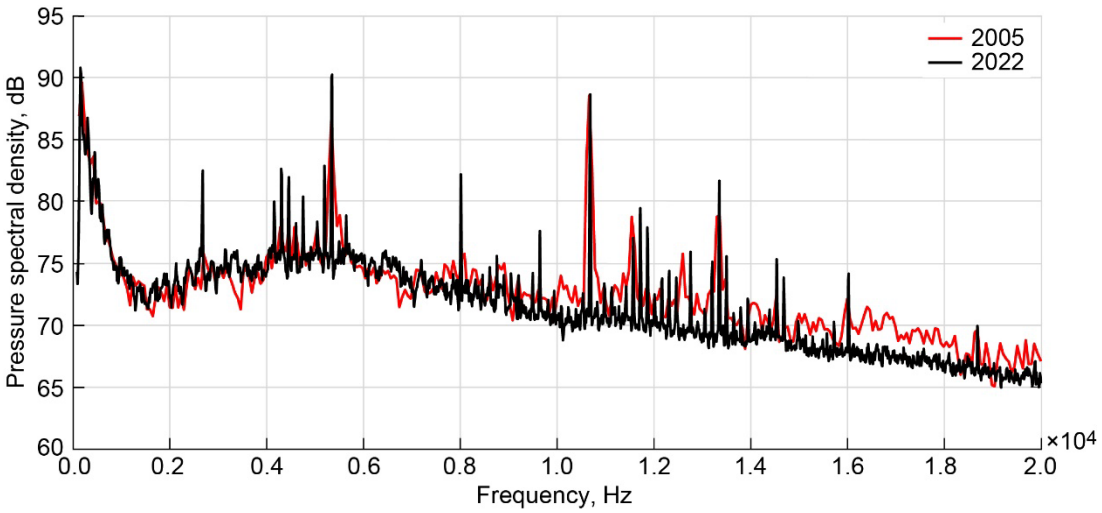

Figure 26.—Comparison of radiated sound pressure spectral densities.

Acoustics

The acoustic instrumentation was very similar between the two tests, in that a ¼-in. condenser microphone was traversed on an 89-in. sideline (four diameters) parallel to the model. The data acquisition procedure is essentially captured in the report by Brown and Stephens (Ref. 10). A new traverse was used in 2022, as mentioned previously. Microphone data was acquired with the traverse continuously moving in C003 (2022); in D065 (2005), the process was to stop at 48 points along the sideline and acquire microphone data while stationary. The data for C003 was recorded in time histories and digitally processed into 12.2 Hz bin width spectra. During 2005 (D065), the data system calculated spectra during acquisition at 59 Hz bin width and the time history was not saved.

As an example of the recorded acoustic data, spectra from 100 percent rpmc speed and a directivity angle of 120° is shown in Figure 26 for both new and legacy tests. Specifically, these are readings 1320 and 265 from D065 and C003, respectively. This comparison is largely qualitative, but it can be seen that the spectral shapes agree quite closely with only a few decibels of difference. The blade rate tone of 2,671 Hz is evident, as well as harmonics at 5,341, 8,012, and 10,682 Hz.

To look at the sound as a function of sideline location, specific tone and broadband levels were quantified. The separation of tone and broadband from a sound spectra was discussed by Sree and Stephens (Ref. 11). Quantification of tone levels from spectral methods was discussed by Svetgoff, Stephens, and Envia (Ref. 12). Spectral method had to be used because time series were not available for the legacy data.

Results of the post-processing are shown in Figure 27. The broadband directivity of the sound is much smoother than the tones and examples are shown in Figure 27(a), (c), and (d) for the one-third octave bands centered at the blade rate and first two harmonics. This metric integrates over frequency, which removes the effect of the spectral bin width differences between the new and legacy data. Specifically, the 2,520 Hz one-third octave band metric shown in Figure 27(a) is integrated across the frequency bins between 2,245 and 2,829 Hz. The agreement is within 1.5 dB at all angles. Conversely, the first blade rate tone at 2,671 Hz is shown in Figure 27(b). The tone level was calculated by subtracting the broadband spectra from the tone spectra and summing the remaining sound pressure level around the frequency of interest. Gaps in the curves represent measurements where the tone was less than 1 dB above the broadband. The tone directivity varies considerably more than broadband, and looking at individual sideline locations is not a useful comparison. The trends in the tone directivity are similar and some features can be identified, but the tone is

subject to constructive and destructive interference effects, unlike the broadband portion of the signal. The increased resolution offered by the scanning microphone traverse reveals that the sound field was under-resolved by the 48 sideline locations. The benefit of additional aft measurement locations is also evident. These results are shown on a sideline with instrument correction applied but without distance modification or atmospheric attenuation losses restored.

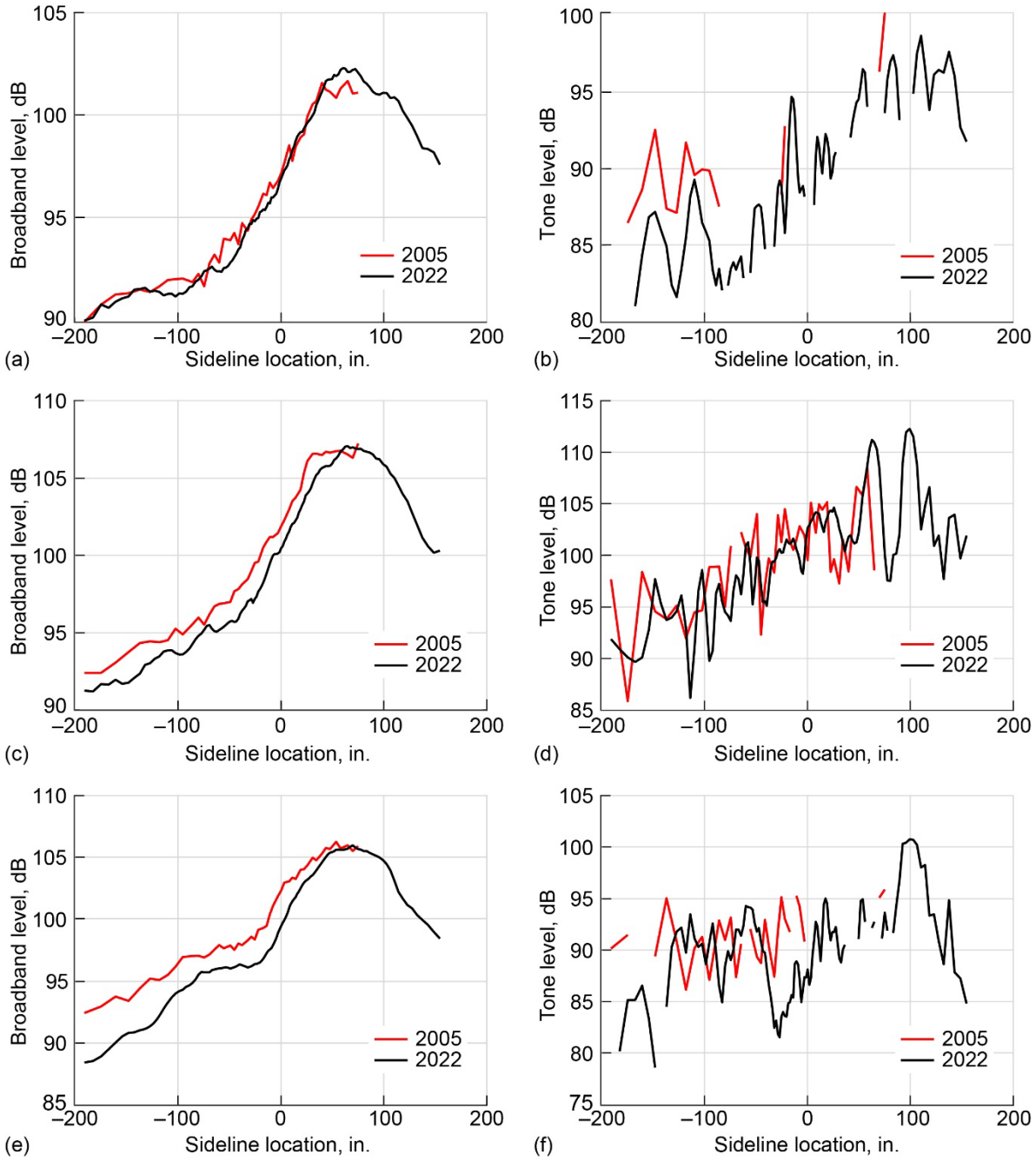

Figure 27.—Comparison of frequency-integrated radiated sound. (a) Broadband level of 2,520 Hz one-third octave band. (b) Tone level of blade rate tone at 2,671 Hz. (c) Broadband level of 5,040 Hz one-third octave band. (d) Tone level of blade rate tone harmonic at 5,342 Hz. (e) Broadband level of 8,000 Hz one-third octave band. (f) Tone level of blade rate tone second harmonic at 8,013 Hz.

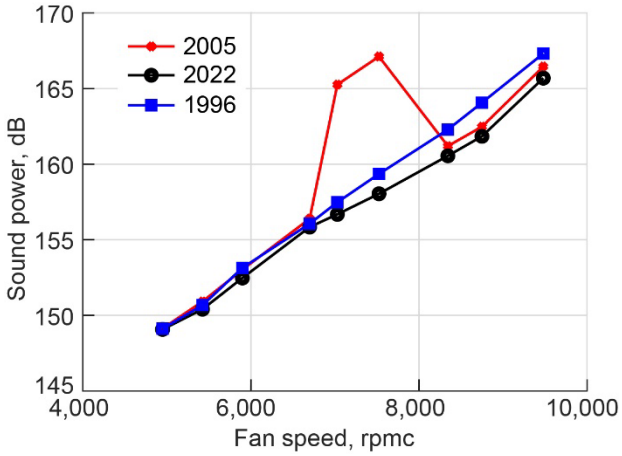

Figure 28.—Radiated sound power.

The integrated metric of sound power is plotted in Figure 28. This combines the spectral frequency and directivity to get a single number for how much sound energy the model is producing. The data from D065 clearly shows an anomaly for two fan speeds, so the earlier data set from D054 (with larger tip gap) was also examined. This shows the data repeats within a few tenths of a decibel. A detailed look at the data set from D065 is beyond the scope of this report. Future reports examining the new data set are anticipated.

Supplemental Data

This report is accompanied by a supplemental data package (TM-20250004035-SUPPL.zip) that is available for download. The data set has several parts, which are described in the following sections.

Aerodynamic Data

The steady aerodynamic performance data is available in a file called “AeroData.txt” containing 83 variables for 206 readings. This includes all of the readings listed in Table 4, along with some zero readings acquired before the tunnel was started for the various runs. The variable names and their descriptions are given in Table 6.

TABLE 6.—COBRA VARIABLE NAMES

Name	Description
Reading	COBRA Reading Number
Date	Date of Reading
Time	Time of Reading
Samples	Number of samples averaged into Reading
RPM	Shaft rate, revolutions per minute
RPMC	RPM divided by total temperature ratio
RPMCK	RPMC divided by 1,000
PCTRPMC	RPMC as percent of 100%
RAARPT12	Ratio of area averaged total pressure at station 12 to the reference test section total pressure
RAARTT12	Ratio of area averaged total temperature at station 12 to the reference test section total temperature

TABLE 6.—COBRA VARIABLE NAMES

Name	Description
EADARTTO	Adiabatic Efficiency using preceding two parameters
WFC	Corrected total weight flow, lbm/s
WBC	Corrected bypass weight flow, lbm/s
WCC	Corrected core weight flow, lbm/s
BPR	Ratio of preceding parameters
MCI	Mach number at core inlet
RMARPT12	Ratio of momentum average total pressure at station 12 to the reference test section total pressure
RMARTT12	Ratio of momentum average total temperature at station 12 to the reference test section total temperature
EADMATTO	Adiabatic efficiency using preceding two parameters (RMARTT12 and RMARPT12)
EADATTCI	Adiabatic efficiency using following two parameters
RAARPTCI	Ratio of area averaged pressure at core inlet to the reference test section value
RAARTTCI	Ratio of area averaged temperature at core inlet to the reference test section value
RMARPTCI	Ratio of momentum averaged pressure at core inlet to the reference test section value
RMARTTCI	Ratio of momentum averaged temperature at core inlet to the reference test section value
EADATTCW	Adiabatic efficiency using following two parameters
RAARPTCW	Ratio of area averaged pressure at core weight flow station to the reference test section value
RAARTTCW	Ratio of area averaged temperature at core weight flow station to the reference test section value
RMARPTCW	Ratio of momentum averaged pressure at core weight flow station to the reference test section value
RMARTTCW	Ratio of momentum averaged temperature at core weight flow station to the reference test section value
VTIPC	Fan tip velocity based on tip radius and shaft rate, ft/s
VAXIAL	Axial flow velocity based on weight flow and area at fan face, ft/s
VHELI	Velocity triangle generated from preceding two values (VTIPC and VAXIAL), ft/s
MTIP	Fan tip Mach number based on VTIPC and tunnel total values for calculating speed of sound
MAXIAL	Axial flow Mach number based on VAXIAL and tunnel total values for calculating speed of sound
MHELI	Velocity triangle generated from preceding two values (MTIP and MAXIAL)
PT450V	Turbine supply total pressure measured at venturi for weight flow calculation, psi
PS450V	Turbine supply static pressure measured at venturi for weight flow calculation, psi
TT450V	Turbine supply total temperature measured at venturi for weight flow calculation, °F
MTV	Mach in 450 line at venturi
PDRST	Pressure measured in drive strut, psi
V1POS	Valve 1 position, percent open
V3POS	Valve 3 position, percent open
PCV3	Pressure at valve 3, psi
PCV1	Pressure at valve 1, psi
WFTV	Weight flow at turbine venturi, lbm/s
TTQ	Turbine torque from shaft power hp and rpm, ft-lbf
HP	Horsepower from change in enthalpy across turbine and turbine mass flow, hp
HPC	Horsepower corrected to standard day conditions, hp
MTS	Test section Mach based on option chosen from Cal 9×15

TABLE 6.—COBRA VARIABLE NAMES

Name	Description
MBM	Mach number computed by measured conditions at tunnel bellmouth rake
MAFT	Mach number computed by measured conditions at tunnel aft rake
REFPT	Reference total pressure, psi
REFTT	Reference total temperature, °R
APTCRR	Average total pressure measured by cruciform reference rake, psi
ATTCRRR	Average total temperature measured by cruciform reference rake, °R
ATTCRR	Average total temperature measured by cruciform reference rake, °F
MPTCRR	Mach calculated from cruciform reference rake
APTBM	Average total pressure measured by bellmouth rake, psi
APSBME	Average static pressure measured by bellmouth rake and digitized by Optimus data system, psi
PSBM	Static pressure measured at bellmouth rake from dedicated transducer, psi
ATTBM	Average total temperature at bellmouth rake, °R
ATTBMF	Average total temperature at bellmouth rake, °F
APTAFT	Average total pressure measured by aft rake, psi
APSAFTE	Average static pressure measured by aft rake and digitized by Optimus data system, psi
PSAFT	Static pressure measured at aft rake from dedicated transducer, psi
ATTAFT	Average total temperature at aft rake, °R
ATTAFTF	Average total temperature at aft rake, °F
PTTSSR	Total pressure in test section from static rings, psi
PTTSBM	Total pressure in test section from bellmouth rake, psi
PTTSAFT	Total pressure in test section from aft rake, psi
PTTS	Total pressure in test section (chosen from preceding options), psi
PSTSSR	Static pressure in test section from static rings, psi
PSTSBM	Static pressure in test section from bellmouth rake, psi
PSTSAFT	Static pressure in test section from aft rake, psi
PSTS	Static pressure in test section (chosen from preceding options), psi
TTTSSR	Total temperature in test section from static rings, °R
TTTSBM	Total temperature in test section from bellmouth rake, °R
TTTSAFT	Total temperature in test section from aft rake, °R
TTTS	Total temperature in test section (chosen from preceding options), °R
TTTSF	Total temperature in test section (chosen from preceding options), °F
MTSSR	Test section Mach from Cal 9×15 computed using static rings
MTSBM	Test section Mach from Cal 9×15 computed using bellmouth rake
MTSAFT	Test section Mach from Cal 9×15 computed using aft rake

Acoustic Data

A folder of text files called “AcousticData” is provided that contains three text files for each of the acoustic readings (245 to 371) listed in Table 4. The individual files are named “RDG-NNN-##.txt” where NNN corresponds to the reading number and ## is the processing level of the acoustic spectra in

the file. The three processing levels are “11,” corresponding to narrowband “as-measured” microphone measurement, “21” means narrowband “instrument corrected” and “41” is the “1-foot lossless” spectra. These spectra are all in units of pressure spectral density referenced to 20 μPa. Details about the methods used for processing acoustic data are given in Reference 10.

The structure of each file is plain text. The first column is the frequency axis with bin width of 12.2 Hz. The first row gives the location of the measurement microphone corresponding to the spectra provided. For series 11 and 21, this value is the streamwise location in meters, with the fan stacking axis at 0 and positive downstream. For series 41, this value is the geometric angle location where positive is downstream. Emission angles can be calculated using Equation (3) in Reference 10, along with the tunnel Mach number for the specific reading. Only the center traverse microphone has been provided in the current data set as this particular fan model is symmetric and no angle-of-attack testing was conducted.

A file containing an in-flow microphone measurement of the empty 9×15 LSWT is also provided as “Empty_9x15_2020.txt.” This has the same format as the fan test acoustic data, where the first column is the frequency vector and the other columns correspond to Mach numbers of 0.05, 0.1, 0.15, 0.20 and 0.22. The self-noise of the test section is spatially uniform.

Fan Geometry Package

A distribution package of flow lines and overall parameters was collected for publication along with this report. A folder called “Geometry” contains the ADP Fan 1 geometry in several file formats. The blade geometry is hot shapes at 100 percent design speed. The purpose of this distribution is to support turbomachinery simulations and comparison with experimental data.

A text-file-based format for the blades in CFX format along with nacelle and core flow lines is given as “ADP_Fan1.zip.” Users should be able to convert these files into other formats for their needs. The same text files were used to produce a SolidWorks assembly by lofting a surface through the individual airfoil profiles. This assembly is given in “ADP_Fan1_SW.zip” and is shown in Figure 29.

Major dimensions of the ADP fan model are shown in Figure 30.

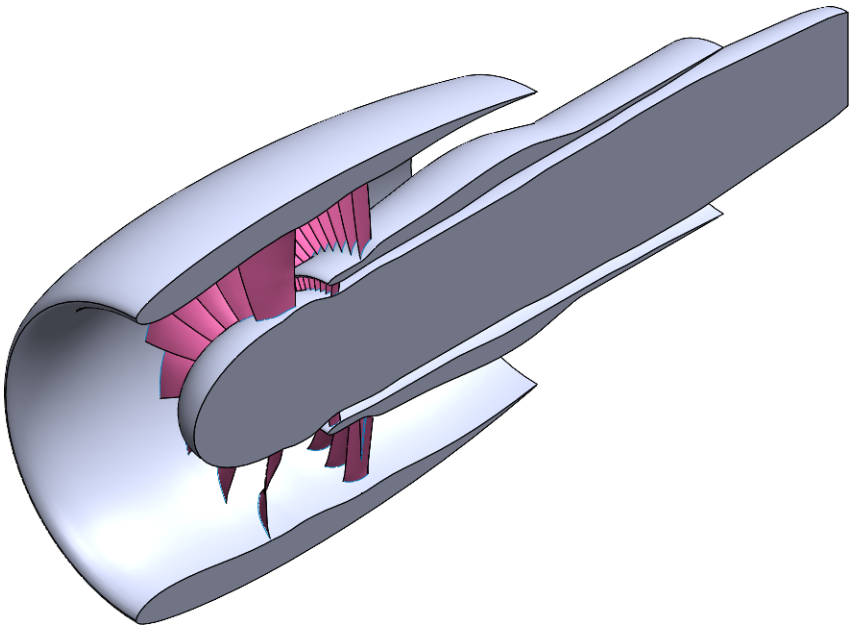

Figure 29.—ADP Fan 1 geometry for simulation purposes.

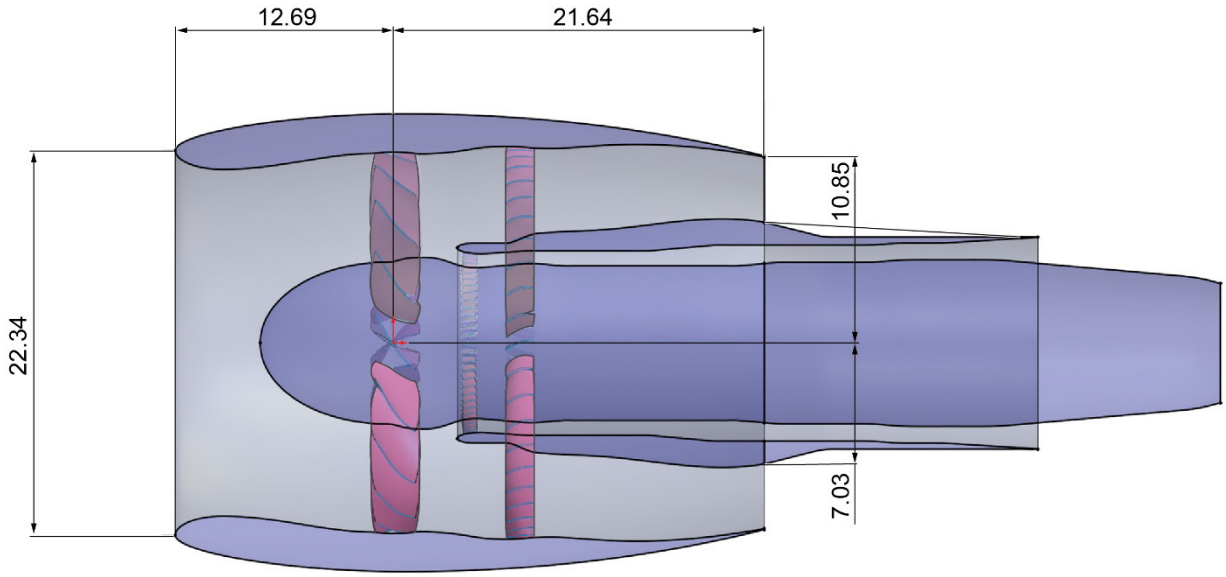

Figure 30.—Major dimensions of the ADP Fan 1 model (all units are inches).

References

1. Stephens, David Bruce, et al.: 9- by 15-Foot Low-Speed Wind Tunnel Acoustic Upgrade—Part 1: Supporting Studies. NASA/TM-20210024786/PART 1, 2022. https://ntrs.nasa.gov
2. Stephens, David Bruce, et al.: 9- by 15-Foot Low-Speed Wind Tunnel Acoustic Upgrade—Part 2: Improvement Comparison. NASA/TM-20210024786/PART 2, 2022. https://ntrs.nasa.gov
3. Jeracki, Robert J.: Comprehensive Report of Fan Performance From Duct Rake Instrumentation on 1.294 Pressure Ratio, 806 ft/sec Tip Speed Turbofan Simulator Models. NASA/TM—2006-213863, 2006. https://ntrs.nasa.gov
4. Dittmar, James H.; Elliott, David M.; and Bock, Lawrence A.: Some Acoustic Results From the Pratt and Whitney Advanced Ducted Propulsor—Fan 1. NASA/TM—1999-209049, 1999. https://ntrs.nasa.gov
5. Envia, Ed: Acoustic Power Transmission Loss Through a Ducted Fan. Presented at the AIAA/CEAS Aeroacoustics Conference, Lyon, France, 2016.
6. Balan, Chellappa; and Hoff, Gregory E.: Propulsion Simulator for High Bypass Turbofan Performance Evaluation. SAE Technical Paper 931410, 1993.
7. Van Zante, Dale; and Suder, Kenneth: Environmentally Responsible Aviation: Propulsion Research to Enable Fuel Burn, Noise and Emissions Reduction. Presented at the International Symposium on Air Breathing Engines, Phoenix, AZ, 2015.
8. Hobbs, David E., et al.: Low Noise Research Fan Stage Design. NASA CR–195382, 1995. https://ntrs.nasa.gov
9. Poljak, Pamela: Uncertainty Analysis of the CE-12 Free-Jet Probe Calibration Facility. NASA/CR-20210023629, 2021. https://ntrs.nasa.gov
10. Brown, Clifford A.; and Stephens, David B.: Acoustic Methods Used in the NASA Glenn 9- by 15-Foot Low-Speed Wind Tunnel. NASA/TM—2018-218874, 2018. https://ntrs.nasa.gov
11. Sree, Dave; and Stephens, David B.: Tone and Broadband Noise Separation From Acoustic Data of a Scale-Model Contra-Rotating Open Rotor. Presented at the AIAA Aeroacoustics Conference, Atlanta, GA, 2014.
12. Svetgoff, Alexander; Stephens, David; and Envia, Edmane: Inlet Radiated Noise Predictions for the NASA Source Diagnostic Test Fan Using Physics-Based Simulations. AIAA 2022–2941, 2022.